Involvement of autophagy-lysosomal degradation in systemic sclerosis

学　位　論　文

Involvement of autophagy-lysosomal degradation in systemic sclerosis

（全身性強皮症におけるオートファジー・リソソーム分解の関与）

福島県立医科大学大学院医学研究科

皮膚粘膜学分野

森　龍彦

Abstract

Autophagy is one of essential intracellular self-degradation systems, and known to maintain the homeostatic balance between the synthesis, degradation and recycling of cellular proteins and organelles. Recently, an association between autophagy and systemic sclerosis (SSc) has been suspected, but the details remain unclear. Therefore, in this study we immunohistologically investigated the expression of an autophagosome marker protein, microtubule-associated protein 1 light chain 3 (LC3), to know the implication of autophagy-lysosome system in the pathogenesis of skin fibrosis/sclerosis observed in scleroderma model mice and SSc patients. In bleomycin (BLM)-injected scleroderma model mice, the number of LC3-positive puncta was significantly higher than that in PBS-injected control mice. As for SSc, more LC3-positive puncta were observed in the lower region of dermis in the sclerotic phase of SSc patients than in controls. On the other hand, such a drastic difference was not observed in the edematous phase of SSc. These results suggest that changes in the autophagy-lysosomal degradation system reflect progression of skin fibrosis in SSc.

Key Word: systemic sclerosis, autophagy, fibrosis, lysosome, LC3

Introduction

Autophagy is one of essential intracellular self-degradation systems, being known to maintain a homeostatic balance between the synthesis, degradation and recycling of cellular proteins and organelles [1, 2, 3]. It is induced by a variety of stress stimuli, such as nutrient starvation, and ischemia, and is initiated with the formation of a double membrane structure, called an isolation membrane, which elongates to enclose the portion of cytoplasm and/or organelles. When the isolation membrane completely closes, it becomes autophagosome, which further acquires lysosomal enzymes by fusion with lysosomes for the degradation of its contents. The resultant structure is called autolysosome. Several Atg (autophagy related gene) proteins, such as Atg5, Atg12, and microtubule-associated protein 1 light chain 3 (LC3), are involved in these steps. Among them, LC3 is known to be recruited on the isolation membrane and the molecules on the inside of the double membrane are degraded and those on the outer membrane are released to the cytoplasm by Atg4. Therefore, LC3 can be a marker of the isolation membranes, autophagosomes, and a fraction of autolysosomes [4, 5, 6, 7].

Impairments of autophagy are often associated with various disease states, such as malignant tumor, heart failure, type 2 diabetes mellitus, and neurodegenerative disease [8, 9, 10, 11, 12]. Recently, it has been reported that autophagy is associated with idiopathic pulmonary fibrosis (IPF) and autoimmune diseases such as systemic lupus erythematosus and rheumatoid arthritis [13, 14, 15]. Systemic sclerosis (SSc) is a multiorgan connective tissue disease characterized by vasculopathy, systemic autoimmunity, and

fibrosis/sclerosis. It has been previously shown that the skin specimens from SSc patients contain more intense LC3 immuno-reactivities than those from healthy controls [16]. However, another report demonstrated that SSc fibroblasts showed impaired autophagy [17]. Therefore, mechanisms of how autophagy-lysosomal system altered in SSc tissues remains elusive. In the present study, we investigated the state of autophagy-lysosomal system in the skin of mouse scleroderma-model and SSc patients.

Method

Mouse samples

Specific pathogen-free C3H/HeJ female mice (6-week old) were purchased from CLEA Japan, Inc. (Tokyo, Japan). They were housed in a controlled environment (21-24°C, 60% humidity, 12-h light/dark cycle), and fed ad libitum. All experimental procedures in this study were approved by the Animal Care and Use Committee of Fukushima Medical University. The scleroderma mouse model was established according to a previous study [18]. Bleomycin (BLM) was obtained from Nippon Kayaku Co. Ltd. (Tokyo, Japan). After filter sterilization, 100 µl of BLM (500 µg/ml) or phosphate-buffered saline (PBS) was intradermally injected into the shaved backs of the mice once daily for 5 days/week, for 2 or 4 weeks. The mice were then divided into four groups (PBS 2 weeks, PBS 4 weeks, BLM 2 weeks and BLM 4 weeks), with n = 5 in each group. Skin samples were biopsied from the injected site.

Human samples

The SSc patients had been diagnosed according to the SSc diagnostic criteria outlined by the Japanese Dermatological Association. They included 5 edematous phase SSc (E-SSc) patients and 5 sclerotic phase SSc (S-SSc) patients, whose clinical characteristics are shown in Table 1. Skin samples were biopsied from their forearm. As controls, skins of benign tumor patients such as epidermal cyst and verruca vulgaris, were biopsied from the forearm. All experimental procedures in this study were approved by the Ethics Committee of Fukushima Medical University.

Immunohistological analyses

The samples were paraffin-embedded and sectioned at 3 μm thickness, which were then deparaffinized and rehydrated. For evaluation of skin fibrosis, the sections were stained with hematoxylin and eosin (HE) or anti-α smooth muscle actin (αSMA) antibody. For the immunohistochemistry of αSMA, the section was incubated with 3% hydrogen peroxide in methanol, and then blocked with 10% normal goat serum (Nichirei Biosciences, 426042). Next, the section was incubated with the anti-αSMA antibody (Abcam, ab7817) at a dilution of 1:100 in an antibody diluent (Roche Diagnostics, 251-018) for 1.5 h at room temperature, followed by the incubation with a mixture of peroxidase-conjugated goat anti-mouse and anti-rabbit IgGs (Nichirei Biosciences, 424151, Simple Stain MAX PO [MULTI]) for 30 min at room temperature. Color development was performed in a solution containing 0.12 mg/ml diaminobenzidine and 0.02% hydrogen peroxide. The sections

were counterstained with hematoxylin. For immunohistofluorescence, the sections were blocked with 5% normal donkey serum (Jackson, 017-000-121), and incubated overnight with rabbit monoclonal antibody against LC3A (Abcam, ab52768; at a dilution of 1:400 in the blocking solution) and mouse monoclonal antibody for αSMA (Abcam; at a dilution of 1:400 in the blocking solution) at 4°C. As secondary antibodies, donkey anti-rabbit IgG conjugated with a fluorescent dye, Alexa Fluor 488 (Jackson, 711-545-152), and donkey anti-mouse antibody conjugated with Alexa Fluor 594 (Jackson, 715-585-150) were used. Hoechst 33342 (Invitrogen, H3570) was used as nuclear staining. The sections were washed with PBS containing 0.1% Tween-20. They were viewed with a laser scanning confocal microscope, FV1000 (Olympus, Japan). For quantification, five regions of interest (ROI) with 105 x 105 μm were randomly captured in the dermis of the mice, and in the upper and lower dermis of the patients. The number of LC3-positive puncta was counted in the ROI, while excluding the area of blood vessels, hair follicles, nerves, and arrector pili muscles. The values were further divided by the number of nuclei in the ROI.

Statistical analysis

All of the data were expressed as box-and-whisker plot and analyzed using EZR software (version 1.35; Saitama Medical Center, Jichi Medical University, Japan) [19]. Statistical difference was evaluated by the Mann-Whitney *U* test or the Steel Dwass test. $P < 0.05$ was considered statistically significant.

Results

LC3-positive puncta in BLM-treated mouse skin

By HE-staining, apparent dermal fibrosis was observed after 4-week treatment of BLM compared to control PBS, but the difference was not so evident after 2-week treatment (Figure 1A-D). αSMA-positive myofibroblasts were detected more often in the dermis from 4 weeks of BLM-treated mice compared to PBS-treated mice, but the difference was not significant after 2 weeks of treatment (Figure 1E-H). Therefore, we conclude that the BLM-induced fibrosis was successful after 4 weeks of the treatment.

We next performed immunohistofluorescence microscopy using anti-LC3 antibody. It was firstly confirmed that this antibody labeled autophagy-related structures, because the number of LC3-positive puncta increased in the starved mouse liver compared to fed mouse liver (Figure 2A). In BLM-treated mice, LC3-positive puncta were often observed in dermal cells (Figure 2C). When the number of LC3-positive puncta per cell was counted, it was significantly higher in BLM-treated mice than in PBS-treated mice after 4 weeks of treatment ($P < 0.05$ in Mann-Whitney U test, n=5; Figure 2D). However, there was no significant difference between them after 2 weeks of treatment.

Additionally, we evaluated mouse treated with BLM together with Ki16425 that is an antagonist for lysophosphatidic acid (LPA) receptors, LPA_1 and LPA_3, and has been previously reported to inhibit dermal fibrosis in BLM-induced scleroderma model mice [20]. The inhibitory effect of the reagent on

the fibrosis was observed by HE-staining, and the number of LC3-positive puncta was low and similar to those in PBS-treated mice (Figure 2E).

LC3-positive puncta in SSc patients

HE-analysis revealed that dermal fibrosis in S-SSc was more severe than that in E-SSc (Figure 3A and B), and collagen bundles in the lower dermis were denser than the upper dermis both in E-SSc and S-SSc (Figure 3A and B). As shown in Figure 3C and D, numerous αSMA-positive myofibroblasts were observed in the lower dermis of the S-SSc specimens, while they were hardly detected in the upper dermal region of S-SSc or any dermal region of E-SSc. In immunohistofluorescence for LC3, a few punctate signals were observed in some dermal cells in the control and E-SSc specimens (Figure 4A and B). Notably, however, dermal cells in S-SSc appeared to contain more LC3-positive puncta than those in other specimens (Figure 4C). When counted, the number in the lower region of S-SSc was significantly higher than the same region of control ($P < 0.05$ in Steel Dwass test; Figure 4D) or than the upper region of S-SSc. ($P < 0.05$ in Mann-Whitney U test; Figure 4D). On the other hand, there was no significant difference in the upper dermis between the S-SSc, E-SSc, and control specimens.

Discussion

This study demonstrated that dermal cells of BLM-treated mice contained more LC3-positive puncta than the control mice, and that the lower dermis of

S-SSc patients also contained more LC3 positive puncta than the control. These results suggest that the autophagy-lysosomal system is affected by BLM-induced signaling and the progression of SSc pathology. Given that LC3 localizes at isolation membrane, autophagsomes, and a portion of autolysosomes [5, 6, 7], the increase in the number of LC3-puncta reflects the autophagy activation and/or the suppression of lysosomal degradation of LC3. It has previously been reported that autophagy is activated after BLM-treatment in mouse lung tissue and a mouse alveolar epithelial cell line, MLE 12 [21, 22, 23], which are well consistent with the present results of BLM-induced LC3-puncta in the mouse dermis. However, because these studies had not carried out flux assays *in vivo*, it remains unclear if autophagy was really activated in BLM-treated mice. Moreover, it should also be noted that Patel et al., recently showed that autophagy is not activated in the lung of IPF, probably mediated by the action of TGF [15]. Therefore, BLM-induced cellular events *in vitro* and pathological process of SSc *in vivo* may be different. Additional assessments of autophagic activity, for example by examination of phosphorylation of mammalian target of rapamycin, isolation membrane-specific markers, and /or lysosomal markers, should be addressed in future.

The present study pointed out key notions for future pathological analyses on SSc relative to autophagy-lysosomal pathway. First, an antagonist for $LPA_{1,3}$ receptor, Ki16425, appeared to suppress BLM-induced LC3-positive puncta, suggesting the reagent may suppress autophagy. Thus, the cross-talks of the signaling pathways of LPA, BLM, and autophagy might be

important to understand the SSc pathology. Second, the number of LC3-positive puncta increased in the lower dermis of S-SSc, but not of E-SSc or in the upper dermis of either SSc patients. As demonstrated in the present and previous studies, the lower dermis of SSc contains increased collagen bundles, fibronectin and myofibroblasts [24, 25, 26]. Therefore, nutritional insufficiency of fibroblasts in this region may directly induce autophagy or somehow suppress lysosomal degradation. It may also be possible that cellular differentiation into myofibroblasts involves autophagy-lysosomal degradation. In fact, recent report proposed that insufficient autophagy might promote myofibroblast differentiation in IPF patients [27].

It is well known that transforming growth factor-β1 (TGF-β1)/Smad signaling plays a key role in the pathogenesis of SSc [28, 29]. Thus, it has been shown previously that TGF-β expression was enhanced in SSc lesions [30], and postnatal activation of TGF-β signaling in mice caused SSc-like skin fibrosis [31], and the genetic ablation of Smad3 in mice reduced BLM-induced fibrosis and collagen synthesis [32]. Moreover, TGF-β induces the conversion of fibroblast to myofibroblast, which strongly induces collagen synthesis [29]. On the other hand, TGF-β1 has been reported to increase the mRNA expression of several Atgs, such as Beclin 1, Atg5, Atg 7, death-associated protein kinase (DAPK) and LC3 through both Smad-dependent and independent pathway [33, 34, 35]. Also, inhibition of autophagy by chemical antagonists (chloroquine and 3-methyladenine), or knockdown of Atg5 or Atg7 resulted in the attenuation of liver fibrogenesis [36] or transdifferentiation of cardiac myofibroblasts [37]. These lines of evidence

together with the present data indicate intimate links between TGF-ß/Smad pathway, autophagy, and fibrosis. A drawback of the above considerations is that the precise function of autophagy-lysosomal systems in the SSc fibrosis has not been uncovered, which should be crarified in future.

Acknowledgments

The author thanks Masaya Yamamoto (School of Health Care, Uekusa Gakuen University), Naoki Tamura, Satoshi Waguri (Department of Anatomy and Histology in this University), and Toshiyuki Yamamoto (Department of Dermatology in this University) for their kind and careful advice during all the course of this study. I also thank Tomoko Okada and Naoko Suzuki (Department of Dermatology of this University) for their technical assistance, Hajime Iwasa and Masatsugu Orui (Department of Public Health in this University) for their help in statistical analyses, and Eiji Huruno and Hiromichi Annoh (Department of Anatomy and Histology in this University) for their help in the starvation experiment in mice. Finally, I deeply thank all the members of both Department of Dermatology and Department of Anatomy and Histology in this University for their fruitful discussions and kind cooperation.

References

1. de Duve C (2005) The lysosome turns fifty. Nat Cell Biol 7: 847-849.

2. Klionsky DJ (2007) Autophagy: from phenomenology to molecular understanding in less than a decade. Nat Rev Mol Cell Biol 8: 931-937.
3. Duszenko M, Ginger ML, Brennand A, Gualdrón-López M, Colombo MI, Coombs GH, Coppens I, Jayabalasingham B, Langsley G, de Castro SL, Menna-Barreto R, Mottram JC, Navarro M, Rigden DJ, Romano PS, Stoka V, Turk B, Michels PA (2011) Autophagy in protists. Autophagy 7: 127-158.
4. Mizushima N, Yoshimori T, Ohsumi Y (2011) The role of Atg proteins in autophagosome formation. Annu Rev Cell Dev Biol 27: 107-132. doi: 10.1146/annurev-cellbio-092910-154005
5. Mizushima N, Yoshimori T, Levine B (2010) Methods in mammalian autophagy research. Cell 140: 313-326. doi: 10.1016/j.cell.2010.01.028.
6. Mizushima N, Yamamoto A, Matsui M, Yoshimori T, Ohsumi Y (2004) In vivo analysis of autophagy in response to nutrient starvation using transgenic mice expressing a fluorescent autophagosome marker. Mol Biol Cell 15: 1101-1111.
7. Kabeya Y, Mizushima N, Ueno T, Yamamoto A, Kirisako T, Noda T, Kominami E, Ohsumi Y, Yoshimori T (2000) LC3, a mammalian homologue of yeast Apg8p, is localized in autophagosome membranes after processing. EMBO J 19: 5720-5728.
8. Komatsu M, Waguri S, Chiba T, Murata S, Iwata J, Tanida I, Ueno T, Koike M, Uchiyama Y, Kominami E, Tanaka K (2006) Loss of autophagy in the central nervous system causes neurodegeneration in mice. Nature 441: 880-884.
9. Nixon RA (2013) The role of autophagy in neurodegenerative disease. Nat

Med 19: 983-997. doi: 10.1038/nm.3232

10. Nishida K, Kyoi S, Yamaguchi O, Sadoshima J, Otsu K (2009) The role of autophagy in the heart. Cell Death Differ 16: 31-38. doi: 10.1038/cdd.2008.163.

11. Jung HS, Lee MS (2010) Role of autophagy in diabetes and mitochondria. Ann N Y Acad Sci 1201: 79-83. doi: 10.1111/j.1749-6632.2010.05614.x.

12. Mathew R, Karantza-Wadsworth V, White E (2007) Role of autophagy in cancer. Nat Rev Cancer 7: 961-967. doi: 10.1038/nrc2254.

13. Alessandri C, Barbati C, Vacirca D, Piscopo P, Confaloni A, Sanchez M, Maselli A, Colasanti T, Conti F, Truglia S, Perl A, Valesini G, Malorni W, Ortona E, Pierdominici M (2012) T lymphocytes from patients with systemic lupus erythematosus are resistant to induction of autophagy. FASEB J 26: 4722-4732. doi: 10.1096/fj.12-206060

14. Lin NY, Beyer C, Giessl A, Kireva T, Scholtysek C, Uderhardt S, Munoz LE, Dees C, Distler A, Wirtz S, Krönke G, Spencer B, Distler O, Schett G, Distler JH (2013) Autophagy regulates TNFα-mediated joint destruction in experimental arthritis. Ann Rheum Dis 72: 761-768. doi: 10.1136/annrheumdis-2012-201671

15. Patel AS, Lin L, Geyer A, Haspel JA, An CH, Cao J, Rosas IO, Morse D (2012) Autophagy in idiopathic pulmonary fibrosis. PLoS One 7: e41394. doi: 10.1371/journal.pone.0041394

16. Frech T, De Domenico I, Murtaugh MA, Revelo MP, Li DY, Sawitzke AD, Drakos S (2014) Autophagy is a key feature in the pathogenesis of systemic sclerosis. Rheumatol Int 34: 435-439. doi: 10.1007/s00296-013-

2827-8

17. Dumit VI, Küttner V, Käppler J, Piera-Velazquez S, Jimenez SA, Bruckner-Tuderman L, Uitto J, Dengjel J (2014) Altered MCM protein levels and autophagic flux in aged and systemic sclerosis dermal fibroblasts. J Invest Dermatol 134: 2321-2330. doi: 10.1038/jid.2014.69
18. Yamamoto T, Takagawa S, Katayama I, Yamazaki K, Hamazaki Y, Shinkai H, Nishioka K (1999) Animal model of sclerotic skin. I: Local injections of bleomycin induce sclerotic skin mimicking scleroderma. J Invest Dermatol 112: 456-462.
19. Kanda Y (2013) Investigation of the freely available easy-to-use software 'EZR' for medical statistics. Bone Marrow Transplant 48: 452-458. doi: 10.1038/bmt.2012.244
20. Ohashi T, Yamamoto T (2015) Antifibrotic effect of lysophosphatidic acid receptors LPA1 and LPA3 antagonist on experimental murine scleroderma induced by bleomycin. Exp Dermatol 24: 698-702. doi: 10.1111/exd.12752
21. Mi S, Li Z, Yang HZ, Liu H, Wang JP, Ma YG, Wang XX, Liu HZ, Sun W, Hu ZW (2011) Blocking IL-17A promotes the resolution of pulmonary inflammation and fibrosis via TGF-beta1-dependent and -independent mechanisms. J Immunol 187: 3003-3014. doi: 10.4049/jimmunol.1004081.
22. Cabrera S, Maciel M, Herrera I, Nava T, Vergara F, Gaxiola M, López-Otín C, Selman M, Pardo A (2015) Essential role for the ATG4B protease and autophagy in bleomycin-induced pulmonary fibrosis. Autophagy 11: 670-684. doi: 10.1080/15548627.2015.1034409.
23. Yang HZ, Wang JP, Mi S, Liu HZ, Cui B, Yan HM, Yan J, Li Z, Liu H, Hua

F, Lu W, Hu ZW (2012) TLR4 activity is required in the resolution of pulmonary inflammation and fibrosis after acute and chronic lung injury. Am J Pathol 180: 275-292. doi: 10.1016/j.ajpath.2011.09.019.

24. Cooper SM, Keyser AJ, Beaulieu AD, Ruoslahti E, Nimni ME, Quismorio FP Jr (1979) Increase in fibronectin in the deep dermis of involved skin in progressive systemic sclerosis. Arthritis Rheum 22: 983-987.
25. Kissin EY, Merkel PA, Lafyatis R (2006) Myofibroblasts and hyalinized collagen as markers of skin disease in systemic sclerosis. Arthritis Rheum 54: 3655-3660.
26. Ackerman AB (1997) Histologic Diagnosis of Inflammatory Skin Diseases second edition: 706
27. Araya J, Kojima J, Takasaka N, Ito S, Fujii S, Hara H, Yanagisawa H, Kobayashi K, Tsurushige C, Kawaishi M, Kamiya N, Hirano J, Odaka M, Morikawa T, Nishimura SL, Kawabata Y, Hano H, Nakayama K, Kuwano K (2013) Insufficient autophagy in idiopathic pulmonary fibrosis. Am J Physiol Lung Cell Mol Physiol 304: L56-69. doi: 10.1152/ajplung.00213.2012.
28. Leask A, Abraham DJ (2004) TGF-beta signaling and the fibrotic response. FASEB J 18: 816-827.
29. Jinnin M (2010) Mechanisms of skin fibrosis in systemic sclerosis. J Dermatol 37: 11-25. doi: 10.1111/j.1346-8138.2009.00738.x
30. Kulozik M, Hogg A, Lankat-Buttgereit B, Krieg T (1990) Co-localization of transforming growth factor beta 2 with alpha 1(I) procollagen mRNA in tissue sections of patients with systemic sclerosis. J Clin Invest 86: 917-

922.

31. Sonnylal S, Denton CP, Zheng B, Keene DR, He R, Adams HP, Vanpelt CS, Geng YJ, Deng JM, Behringer RR, de Crombrugghe B (2007) Postnatal induction of transforming growth factor beta signaling in fibroblasts of mice recapitulates clinical, histologic, and biochemical features of scleroderma. Arthritis Rheum 56: 334-344.
32. Lakos G, Takagawa S, Chen SJ, Ferreira AM, Han G, Masuda K, Wang XJ, DiPietro LA, Varga J (2004) Targeted disruption of TGF-beta/Smad3 signaling modulates skin fibrosis in a mouse model of scleroderma. Am J Pathol 165: 203-217.
33. Ding Y, Kim JK, Kim SI, Na HJ, Jun SY, Lee SJ, Choi ME (2010) TGF-{beta}1 protects against mesangial cell apoptosis via induction of autophagy. J Biol Chem 285: 37909-37919. doi: 10.1074/jbc.M109.093724
34. Kiyono K, Suzuki HI, Matsuyama H, Morishita Y, Komuro A, Kano MR, Sugimoto K, Miyazono K (2009) Autophagy is activated by TGF-beta and potentiates TGF-beta-mediated growth inhibition in human hepatocellular carcinoma cells. Cancer Res 69: 8844-8852. doi: 10.1158/0008-5472.CAN-08-4401
35. He C, Klionsky DJ (2009) Regulation mechanisms and signaling pathways of autophagy. Annu Rev Genet 43: 67-93. doi: 10.1146/annurev-genet-102808-114910
36. Hernández-Gea V, Ghiassi-Nejad Z, Rozenfeld R, Gordon R, Fiel MI, Yue Z, Czaja MJ, Friedman SL (2012) Autophagy releases lipid that promotes fibrogenesis by activated hepatic stellate cells in mice and in human

tissues. Gastroenterology 142: 938-946. doi: 10.1053/j.gastro.2011.12.044

37. Gupta SS, Zeglinski MR, Rattan SG, Landry NM, Ghavami S, Wigle JT, Klonisch T, Halayko AJ, Dixon IM (2016) Inhibition of autophagy inhibits the conversion of cardiac fibroblasts to cardiac myofibroblasts. Oncotarget 7: 78516-78531. doi: 10.18632/oncotarget.12392

Figure legends

Figure 1. Histological evaluations of BLM-treated mice

Mice were treated with PBS (A, C, E and G) or BLM (B, D, F and H) for 2 weeks (2w, A, B, E and F) or 4 weeks (4w, C, D, G and H). The skins were examined by HE staining (HE, A-D) or immunohistochemistry for αSMA (αSMA, E-H). Boxed region in H is magnified and shown in inset. Arrows in H indicate αSMA-positive myofibroblasts. Scale Bars, 50 μm.

Figure 2. Immunohistofluorescence for LC3 in BLM-treated mice

Mice liver with (Stv) or without (Fed) 24-hour starvation were processed for immunohistofluorescence microscopy using anti-LC3 antibody (red, A). Nuclei are stained with Hoechst (blue). Scale bar, 10 μm. Skins from mice treated with PBS (B) or BLM (C) for 2 weeks (2w) or 4 weeks (4w) were double immunolabeled using anti-LC3 (green) and anti-αSMA (red) antibodies followed by appropriate secondary antibodies. Nuclei are stained with Hoechst 33342 (blue). Boxed regions are magnified and shown on the right. Arrows indicate LC3-positive puncta observed in dermal cells. Scale bars,

10 μm. LC3-positive puncta were counted as described in Materials and Methods and expressed as a box-and-whisker plot in D. "＊" indicates significant difference ($P < 0.05$ in Mann-Whiteny U test). Mice treated with BLM and Ki16425 were examined by HE staining (HE, E) and immunohistofluorescence for LC3 and αSMA (LC3/αSMA, E). Nuclei are stained with Hoechst 33342 (blue). Scale bars, 50 μm in HE and 10 μm in LC3/αSMA.

Figure 3. Histological evaluation of the skins from SSc patients

E-SSc (A and C) and S-SSc (B and D) specimens were examined by HE-staining (HE, A and B) or immunohistochemistry for αSMA (C and D). Upper (Up) and lower (Lo) regions of dermis (boxed) in each low magnification picture are magnified and shown in the bottom, respectively. Arrows in D indicate αSMA-positive myofibroblasts. Scale bars, 100 μm.

Figure 4. Immunohistofluorescence for LC3 in the dermis of SSc patients

Control (A), E-SSc (B) and S-SSc (C) specimens were examined by double-immnostaining for LC3 (green) and αSMA (red). Upper (Up) and lower (Lo) regions of the dermis are shown. Boxed regions are magnified and shown on the right. Arrows indicate LC3-positive puncta observed in dermal cells. Scale bars, 10 μm. LC3-positive puncta were counted as described in Materials and Methods and expressed as a box-and-whisker plot in D. "＊" and "＊＊" indicate significant difference ($P < 0.05$) by Mann-Whiteny U test and Steel Dwass test, respectively.

Figure 1. Histological evaluations of BLM-treated mice.

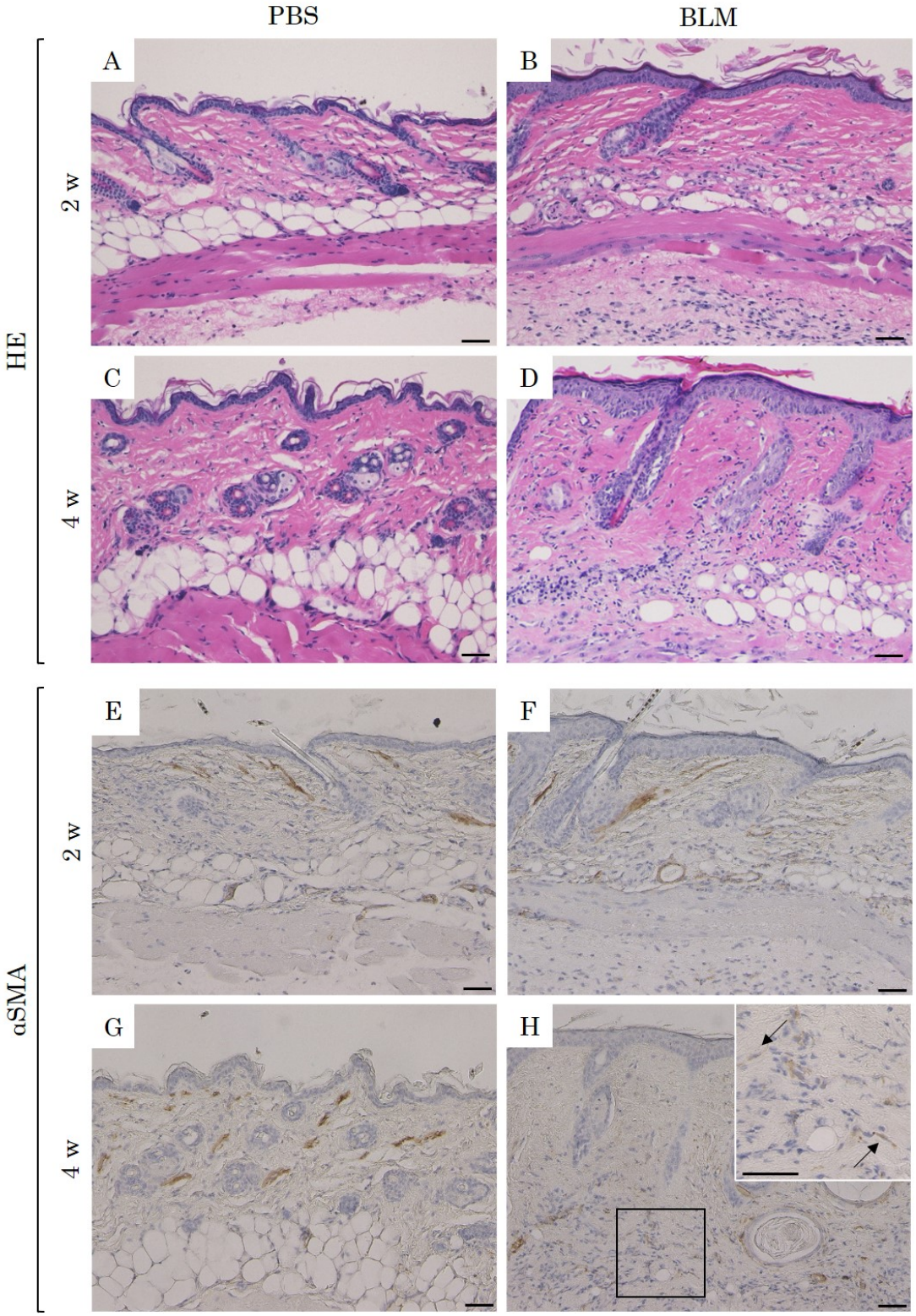

Figure 2. Immunohistofluorescence for LC3 in BLM-treated mice

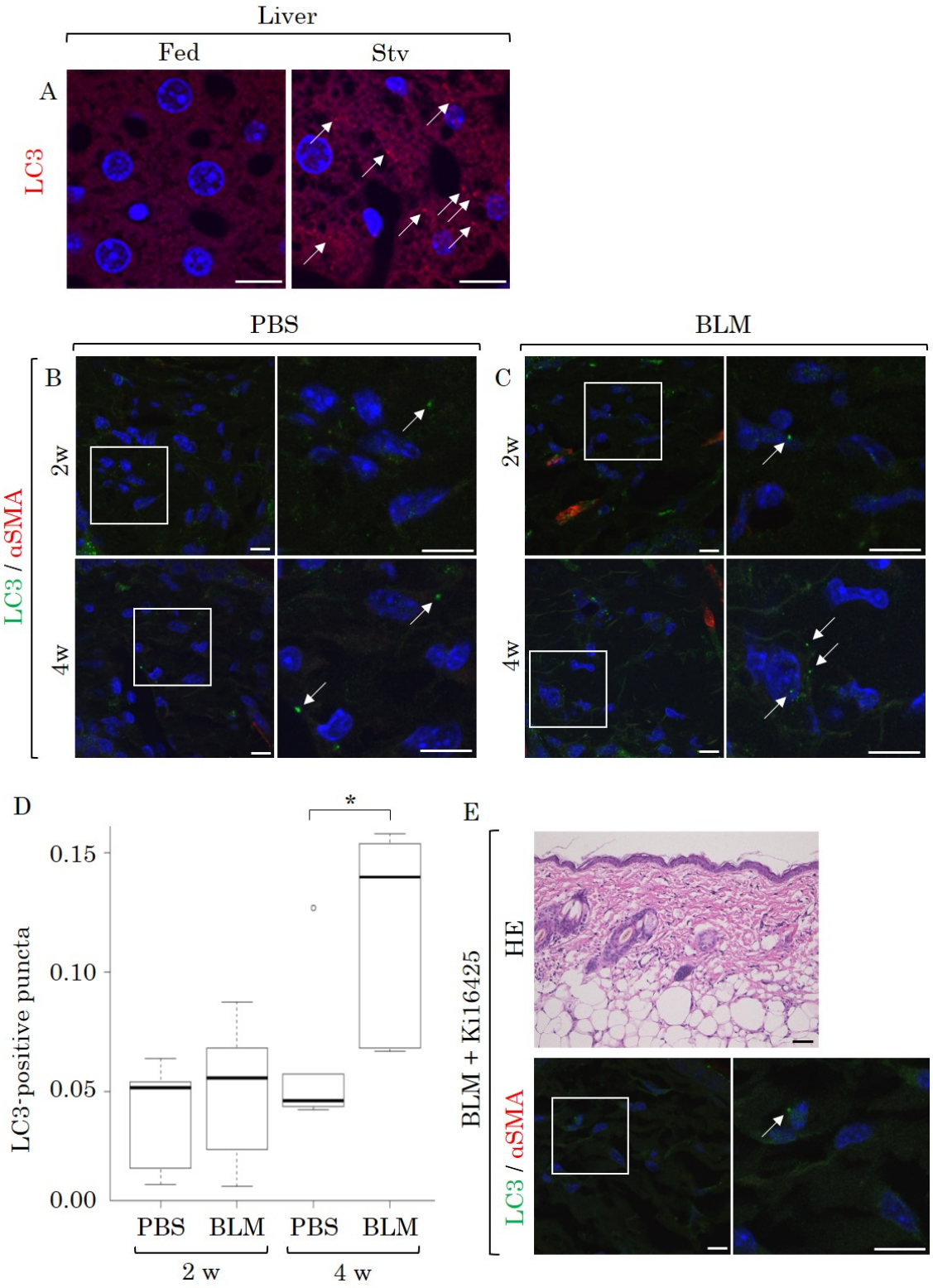

Figure 3. Histological evaluation of the skins from SSc patients

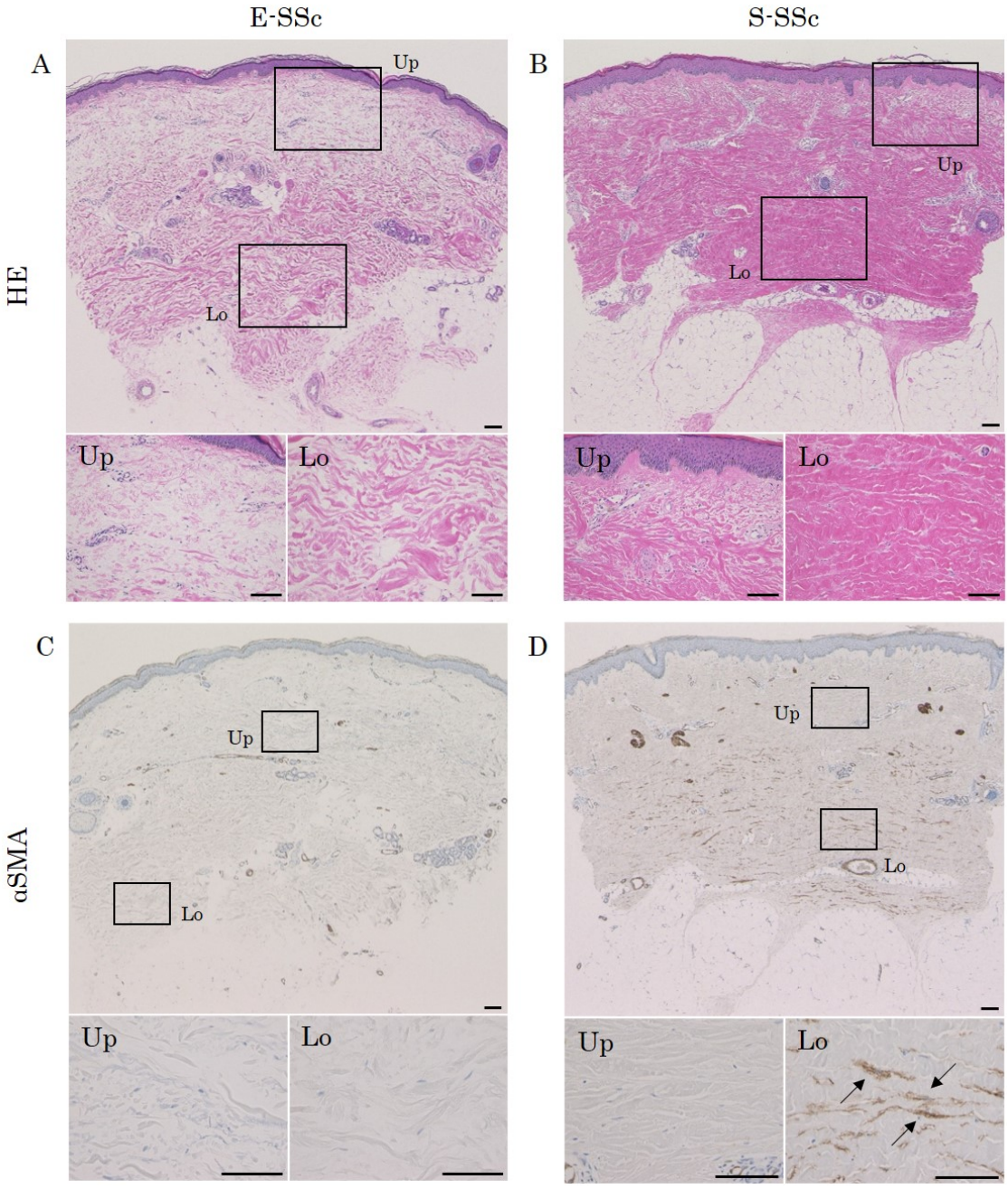

Figure 4. Immunohistofluorescence for LC3 in the dermis of SSc patients

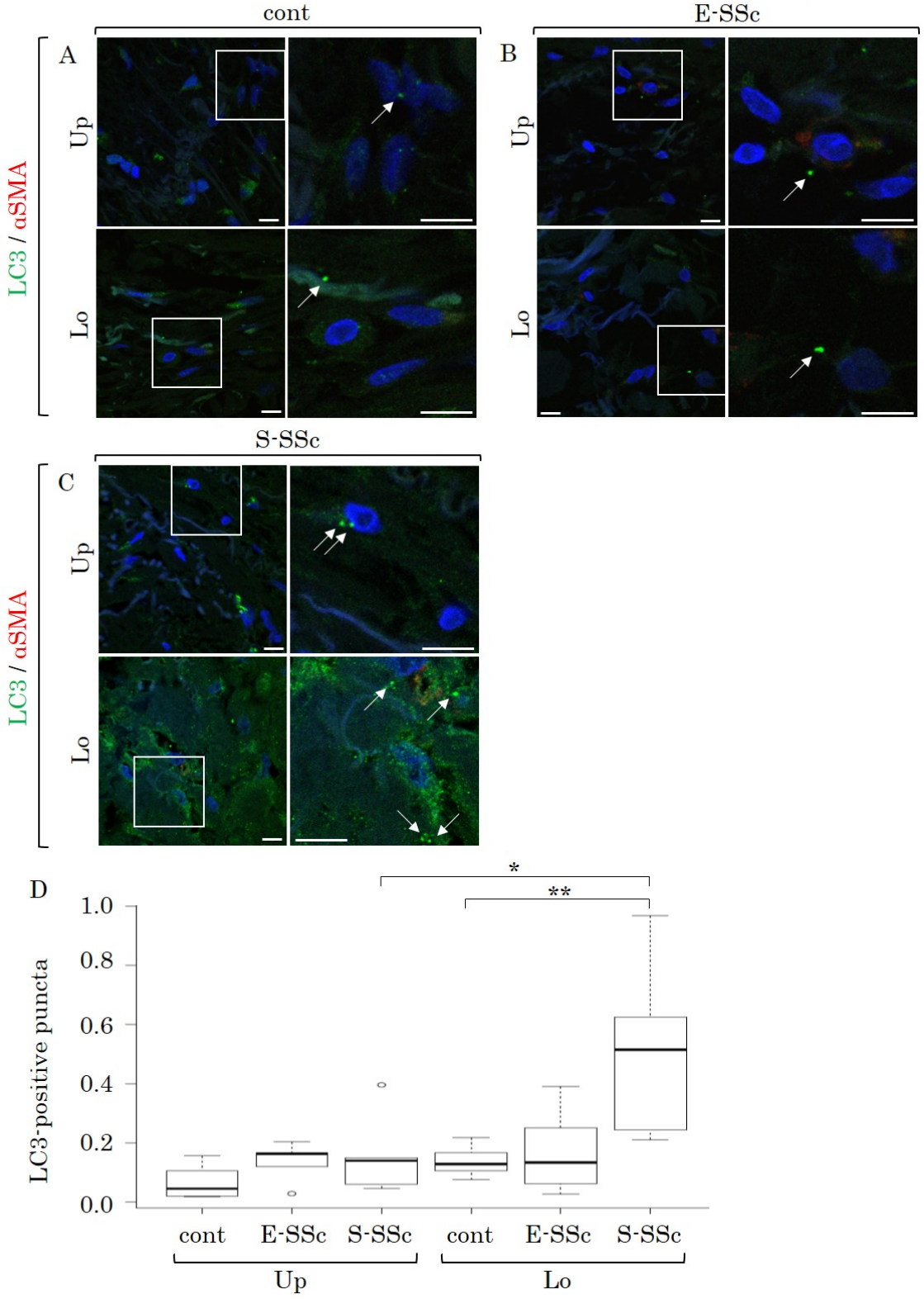

Table 1. Clinical characteristics of SSc patients

SSc type	Age	Sex	Skin symptoms other than skin fibrosis	Autoantibody	Lesions of internal organs	LC3-positive puncta per cell upper dermis	lower dermis
E-SSc	55	F	Raynaud	centromere	-	0.12	0.026
	63	F	Raynaud, nail fold bleeding and extension	-	-	0.164	0.25
	63	F	-	U1-RNP	interstitial lung disease	0.203	0.39
	68	F	nail fold bleeding and extension	centromere	-	0.027	0.133
	79	M	-	centromere	interstitial lung disease, primary biliary cirrhosis	0.163	0.063
S-SSc	7	F	nail fold bleeding and extension, digital ulcer	Scl-70	interstitial lung disease, arthritis, myositis	0.047	0.211
	27	F	Raynaud, nail fold bleeding	U1-RNP	-	0.061	0.243
	47	F	Raynaud, leg livedo	-	interstitial lung disease	0.149	0.625
	51	F	Raynaud, nail fold bleeding	centromere	arthritis	0.14	0.968
	63	M	Raynaud, digital ulcer	-	interstitial lung disease, aortic regurgitation, left ventricular hypertrophy	0.396	0.515